Skolkovo Institute of Science and Technology
Center of Material Technologies

Report on the course

«Numerical Methods in Engineering and Science».

Executor:
PhD Student A.S. Kulikov

Lecturer:
Prof. O.V. Vasilyev

Skolkovo
2023

Contents

Part I

Lagrange and Hermite interpolation

Lagrange and Hermite interpolants are considered for a set of functions and grid distributions in the interval [0, 1]. Functions:

1. $\frac{1}{1+x^2}$.

2. $(x-\frac{1}{2})^2 sign(x-\frac{1}{2})$.

3. $|x-\frac{1}{2}|$.

4. $\sqrt{1-x^2}$.

Corresponding derivatives:

1. $\frac{-2x}{(1+x^2)^2}$.

2. $2(x-\frac{1}{2})sign(x-\frac{1}{2})$.

3. $sign(x-\frac{1}{2})$.

4. $\frac{-x}{\sqrt{1-x^2}}$.

Grid distributions:

1. Equispaced: $x_i = \frac{i}{N}, \quad i = 0, ..., N$.

2. Chebyshev: $\frac{1}{2} - \frac{1}{2}cos(\frac{i}{N}\pi), \quad i = 0, ..., N$.

3. Asin: $\frac{1}{2} + \frac{1}{\pi}sin^{-1}\left(\frac{2i}{N} - 1\right), \quad i = 0, ..., N$.

where N is the number of data points. The error of Lagrange interpolant is majorated by $\frac{\|y^{N+1}\|\|F_N\|}{(N+1)!}$ and of Hermit by $\frac{\|y^{2N+2}\|\|F_N^2\|}{(2N+2)!}$, where $F_N(x) = \prod_{j=0}^{N}(x - x_j)$. Since $\|F_N\|$ is minimal on Chebyshev nodes we expect our interpolation to be the most accurate on them.

1 $\frac{1}{1+x^2}$

1.1 Lagrange interpolant

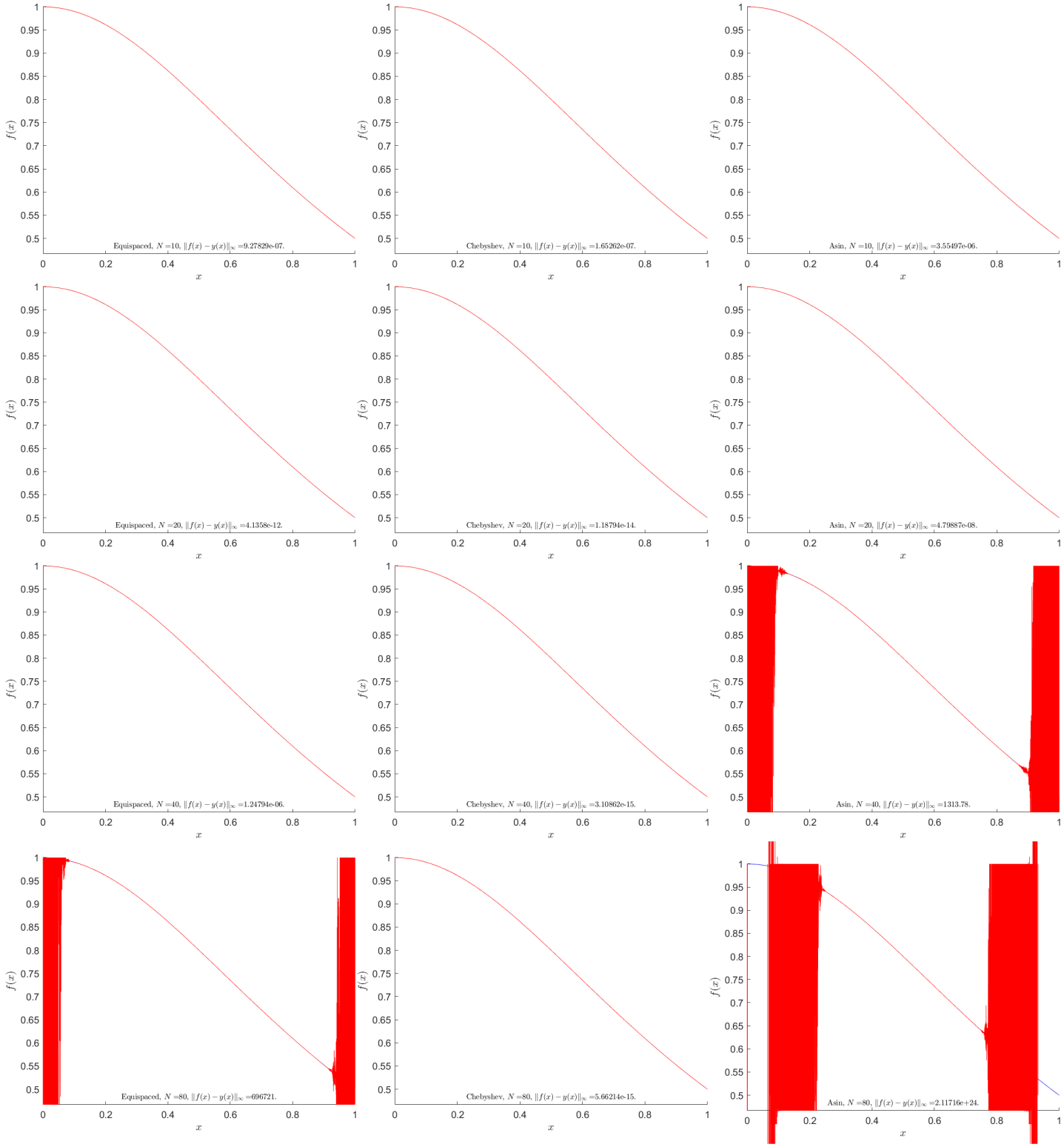

Figure 1. Results of Lagrange interpolation for 10, 20, 40 and 80 data points. The function is pictured with blue, its interpolant with red. First colomn corresponds to Equispaced data point distribution, second to Chebyshev and third to Asin.

1.2 Hermit interpolant

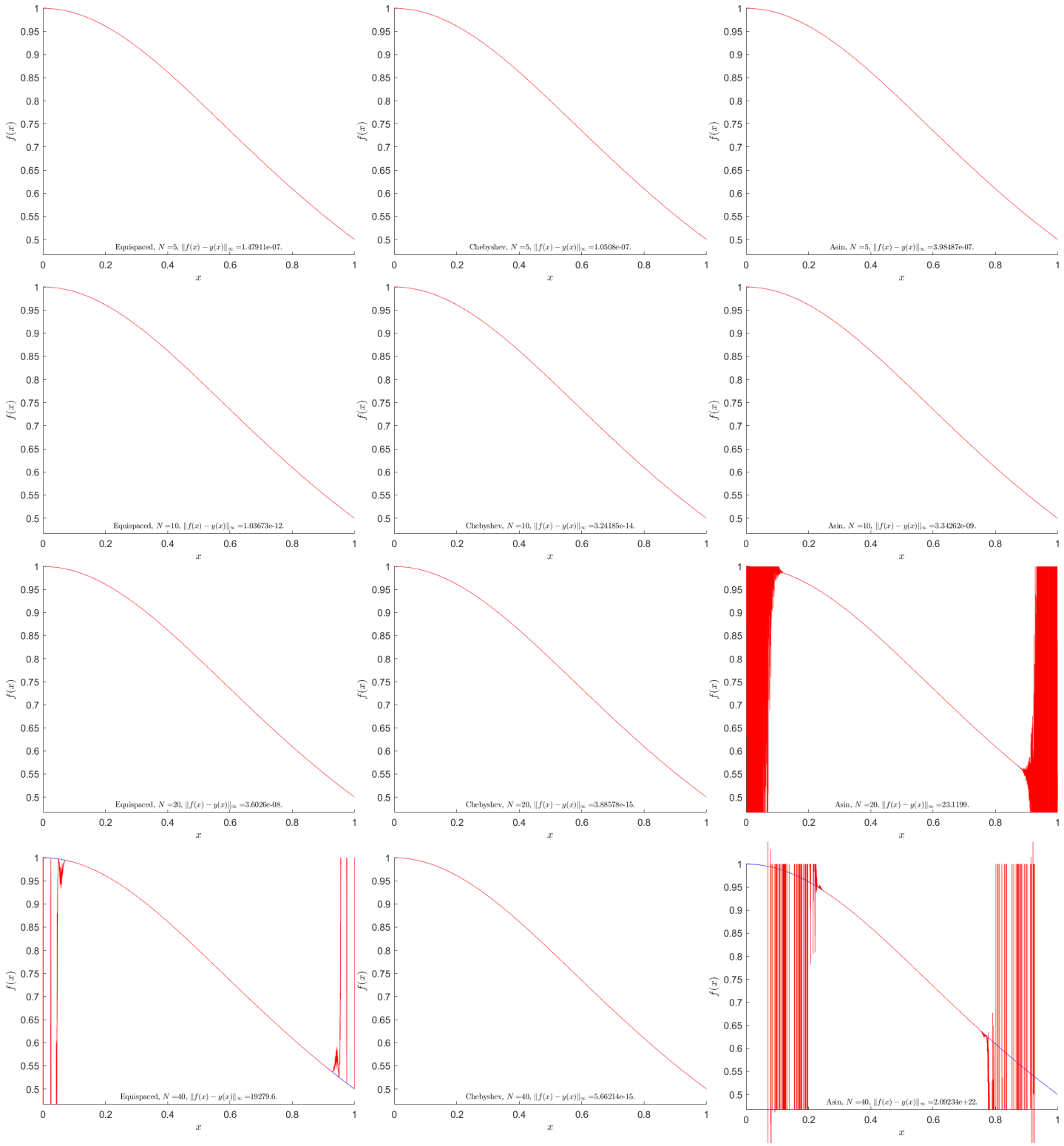

Figure 2. Results of Hermit interpolation for 5, 10, 20 and 40 data points. The function is pictured with blue, its interpolant with red. First colomn corresponds to Equispaced data point distribution, second to Chebyshev and third to Asin.

1.3 Accuracy analysis

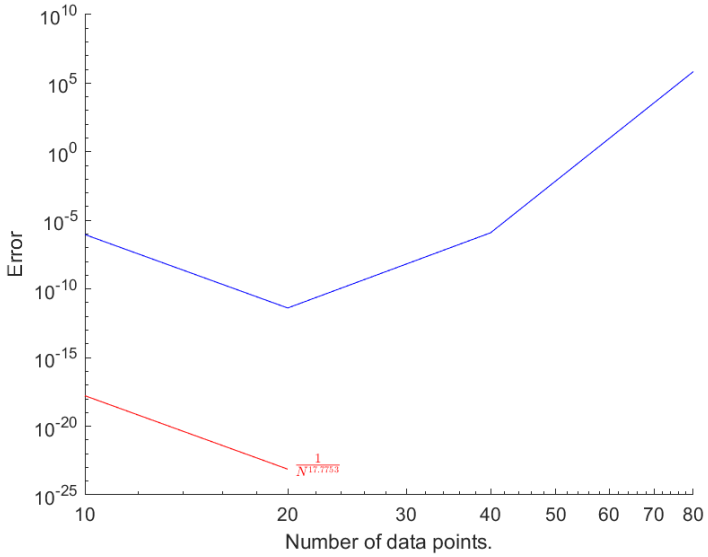

Figure 3. Dependence of error on the number of data points for Lagrange interpolant and Equispaced point distribution.

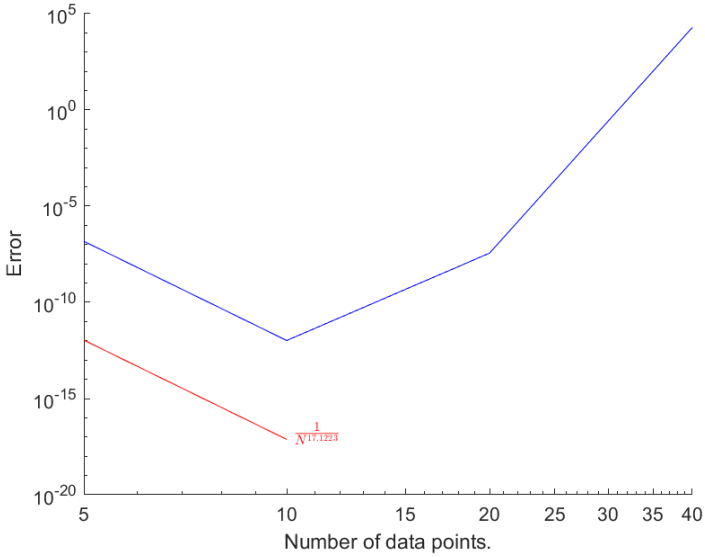

Figure 4. Dependence of error on the number of data points for Hermit interpolant and Equispaced point distribution.

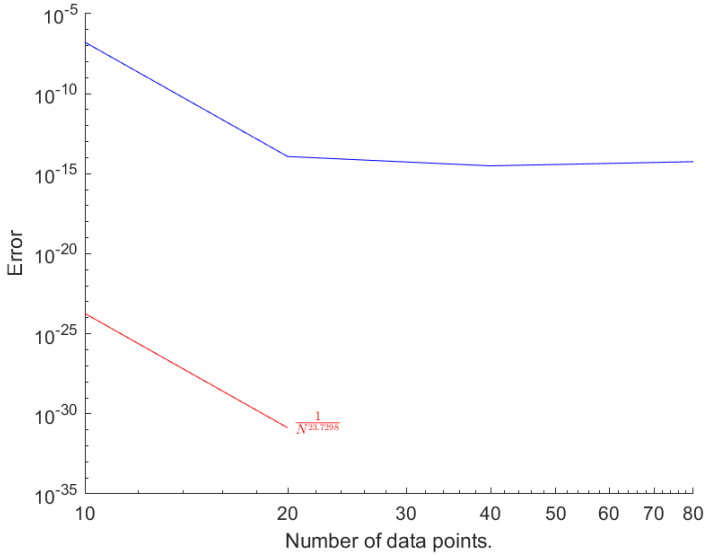

Figure 5. Dependence of error on the number of data points for Lagrange interpolant and Chebyshev point distribution.

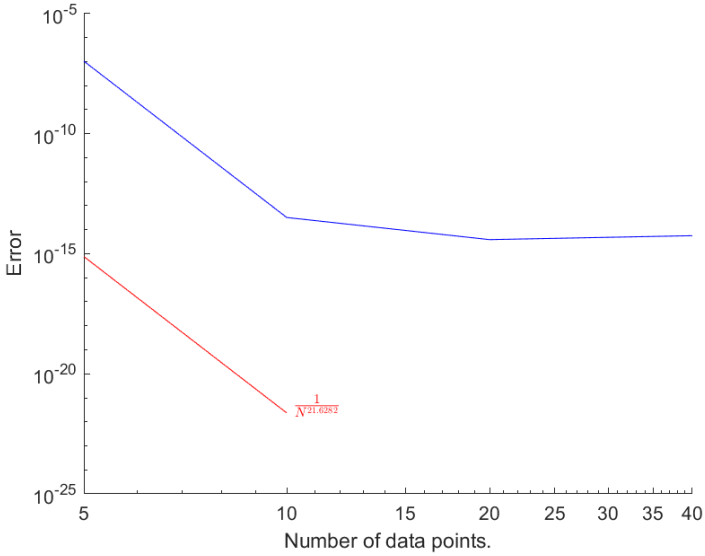

Figure 6. Dependence of error on the number of data points for Hermit interpolant and Chebyshev point distribution.

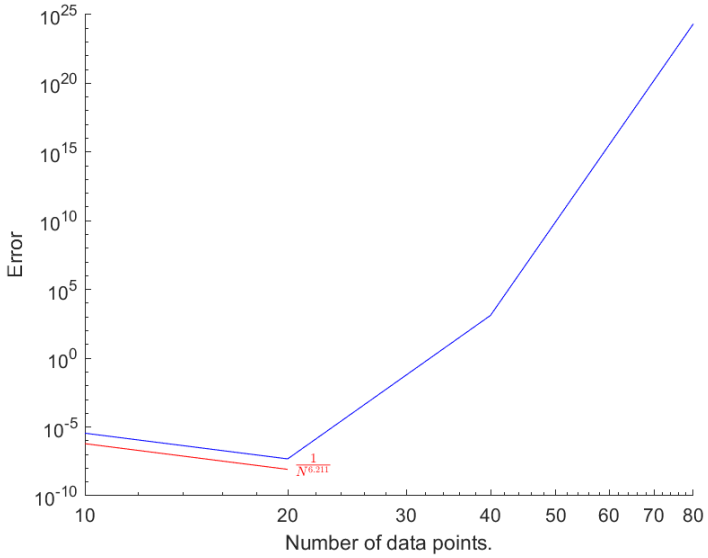

Figure 7. Dependence of error on the number of data points for Lagrange interpolant and Asin point distribution.

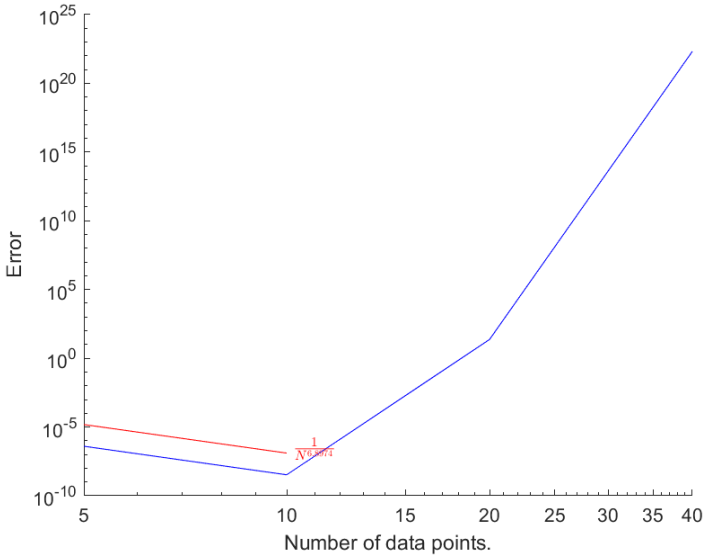

Figure 8. Dependence of error on the number of data points for Hermit interpolant and Asin point distribution.

As expected, Chebyshev point distribution provides the best accuracy. Second best is for Equispaced distribution and the worst is for Asin. Since Chebyshev point distribution is the most accurate and it gets denser the closer the interval boundaries are, it seems logical that Asin is the least accurate, because it gets rarer when approaching them. For this particular function Hermit interpolation turned out to be more accurate than Lagrange. Most likely it is due to the function smoothness. Note that for high N the error grows rapidly, which is not only connected with $\|y^{N+1}\|$ growth, but also with "round-off" error accumulation.

2 $(x-\frac{1}{2})^2 sign(x-\frac{1}{2})$

2.1 Lagrange interpolant

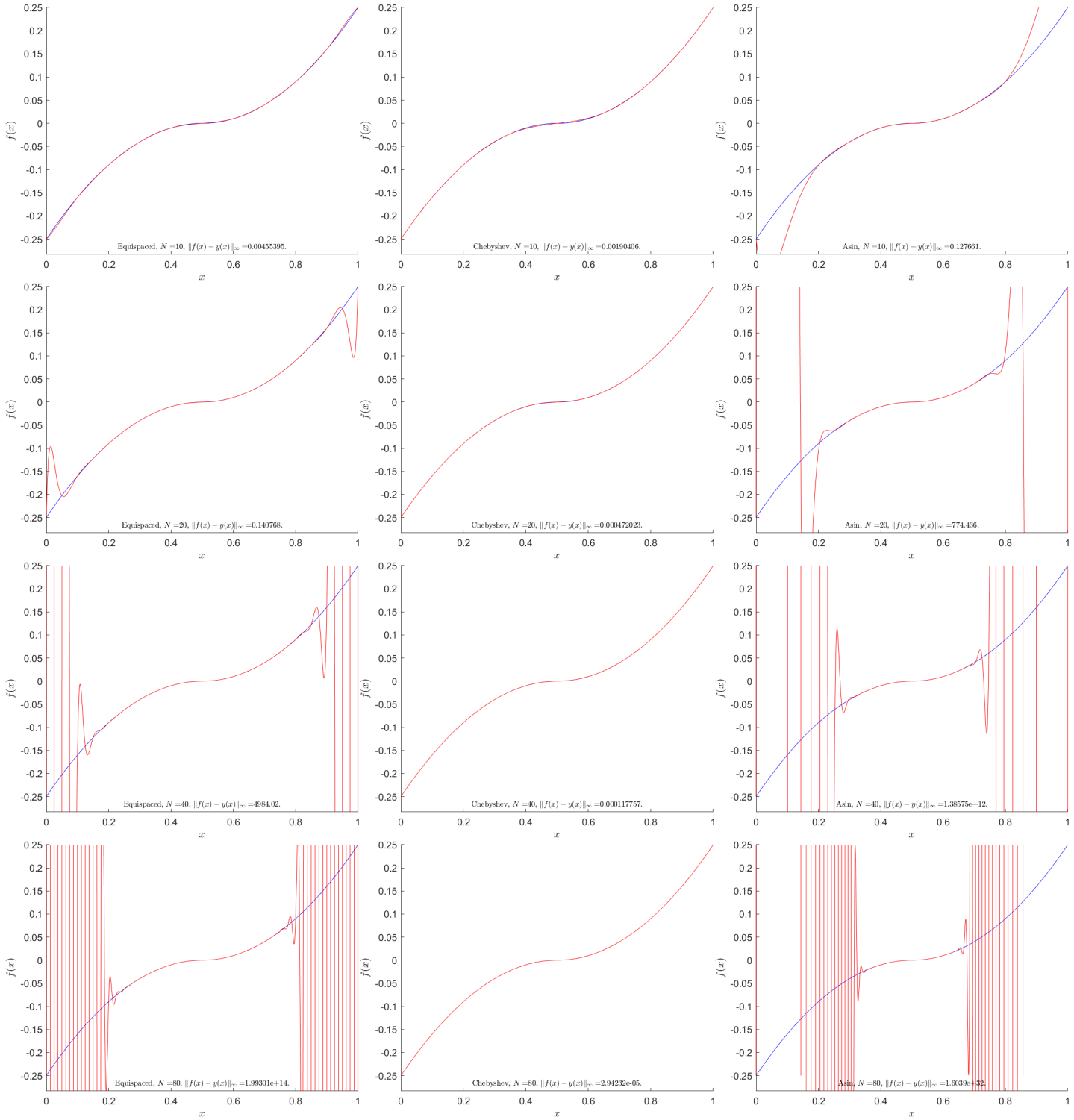

Figure 9. Results of Lagrange interpolation for 10, 20, 40 and 80 data points. The function is pictured with blue, its interpolant with red. First colomn corresponds to Equispaced data point distribution, second to Chebyshev and third to Asin.

2.2 Hermit interpolant

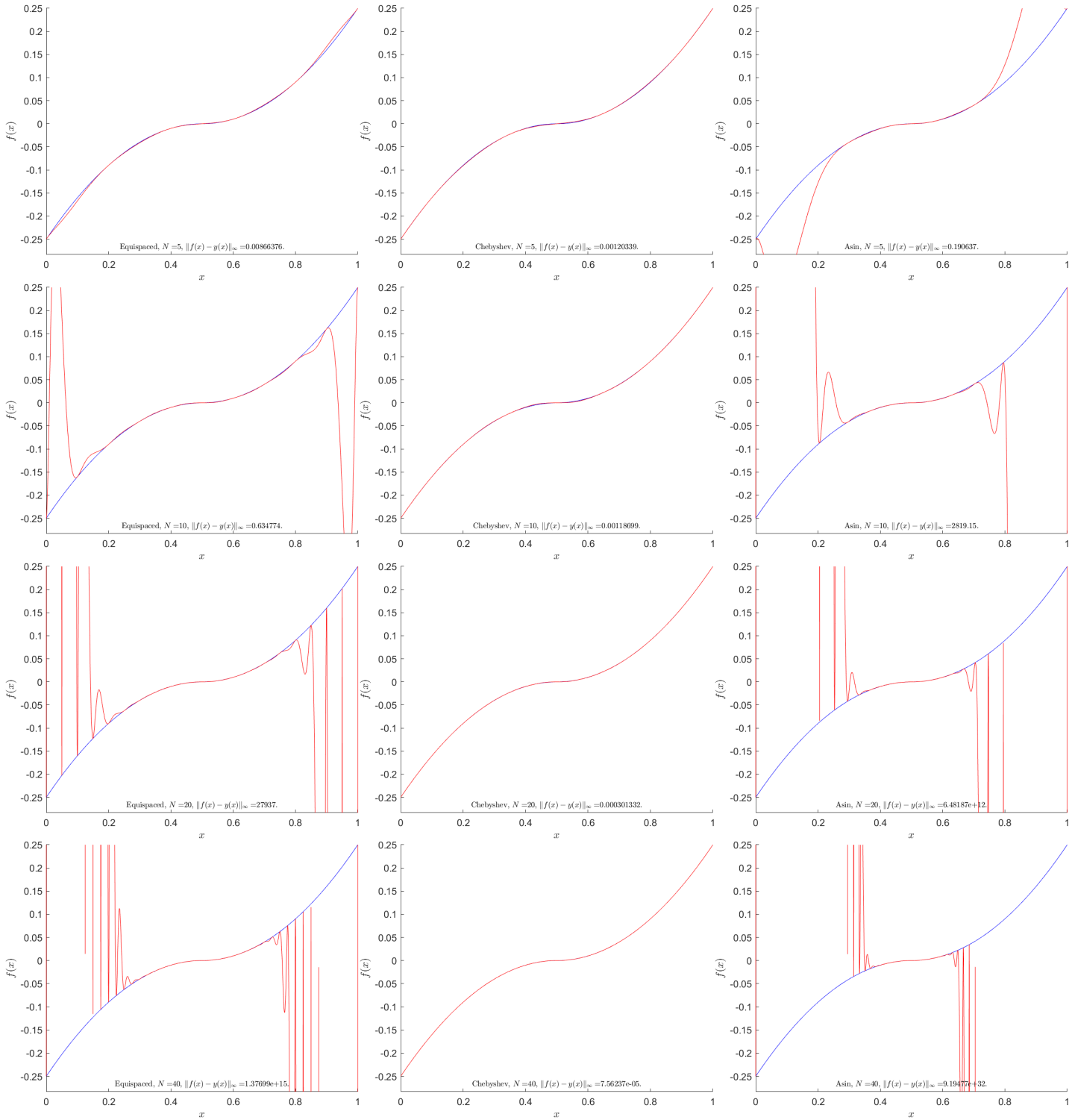

Figure 10. Results of Hermit interpolation for 5, 10, 20 and 40 data points. The function is pictured with blue, its interpolant with red. First colomn corresponds to Equispaced data point distribution, second to Chebyshev and third to Asin.

2.3 Accuracy analysis

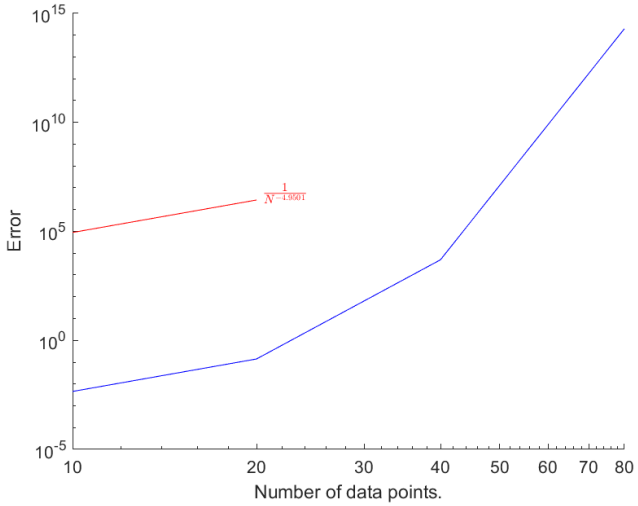

Figure 11. Dependence of error on the number of data points for Lagrange interpolant and Equispaced point distribution.

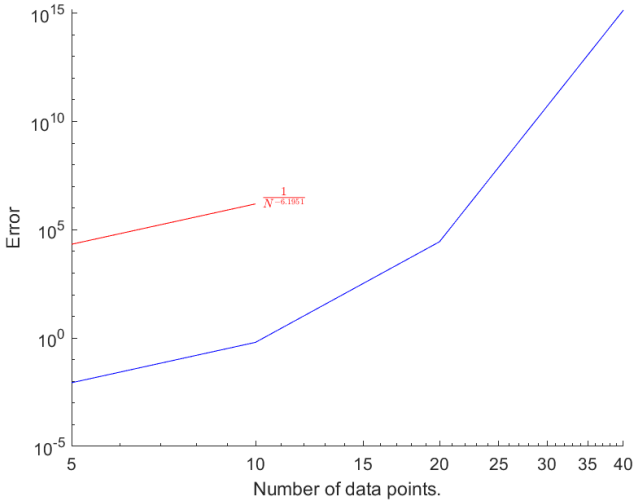

Figure 12. Dependence of error on the number of data points for Hermit interpolant and Equispaced point distribution.

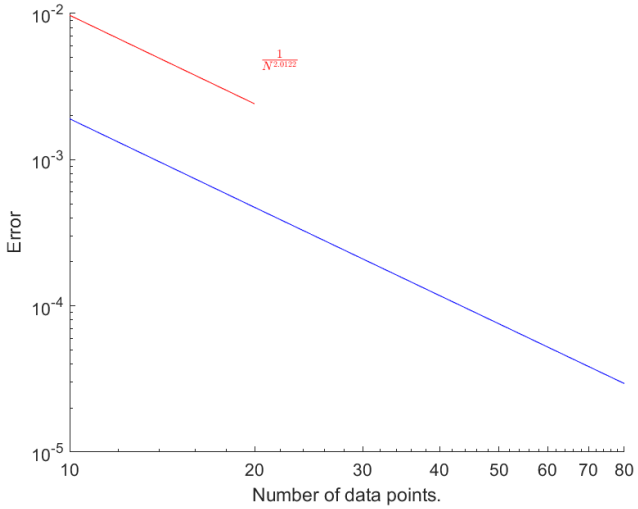

Figure 13. Dependence of error on the number of data points for Lagrange interpolant and Chebyshev point distribution.

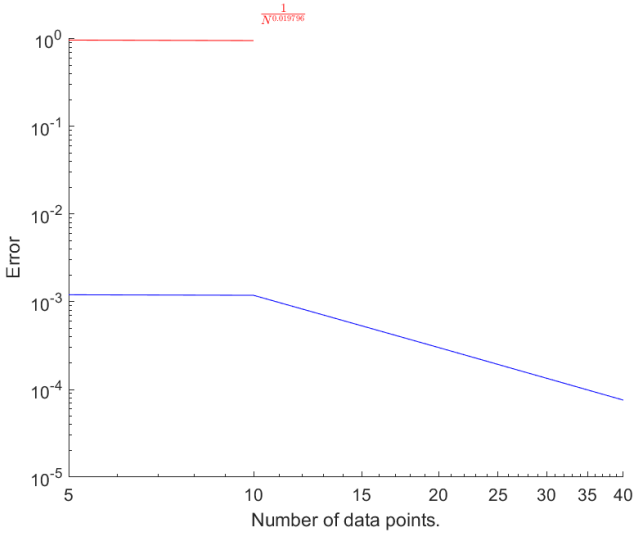

Figure 14. Dependence of error on the number of data points for Hermit interpolant and Chebyshev point distribution.

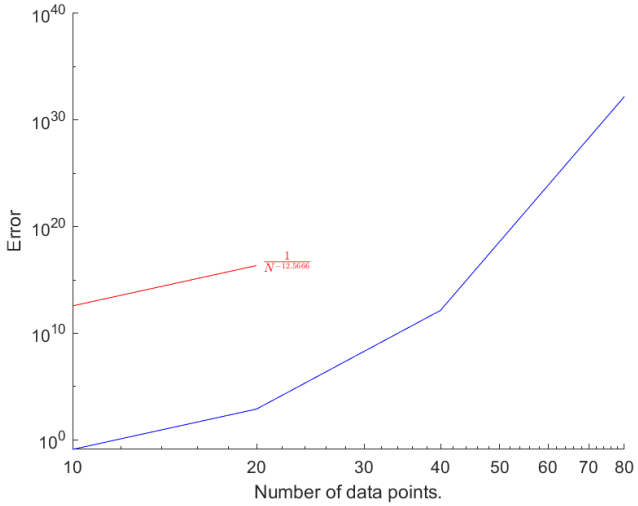

Figure 15. Dependence of error on the number of data points for Lagrange interpolant and Asin point distribution.

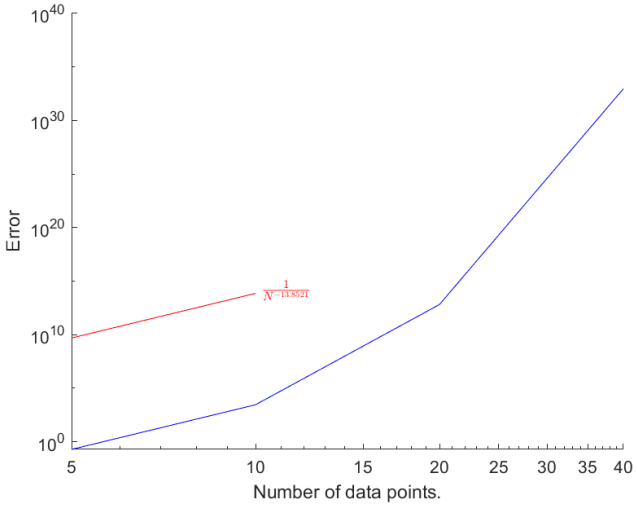

Figure 16. Dependence of error on the number of data points for Hermit interpolant and Asin point distribution.

The accuracy for this function interpolation is significantly smaller. This is because this function is not as smooth as the previous one. For the same reason Lagrange interpolant is more accurate than Hermit.

3 $|x - \frac{1}{2}|$

3.1 Lagrange interpolant

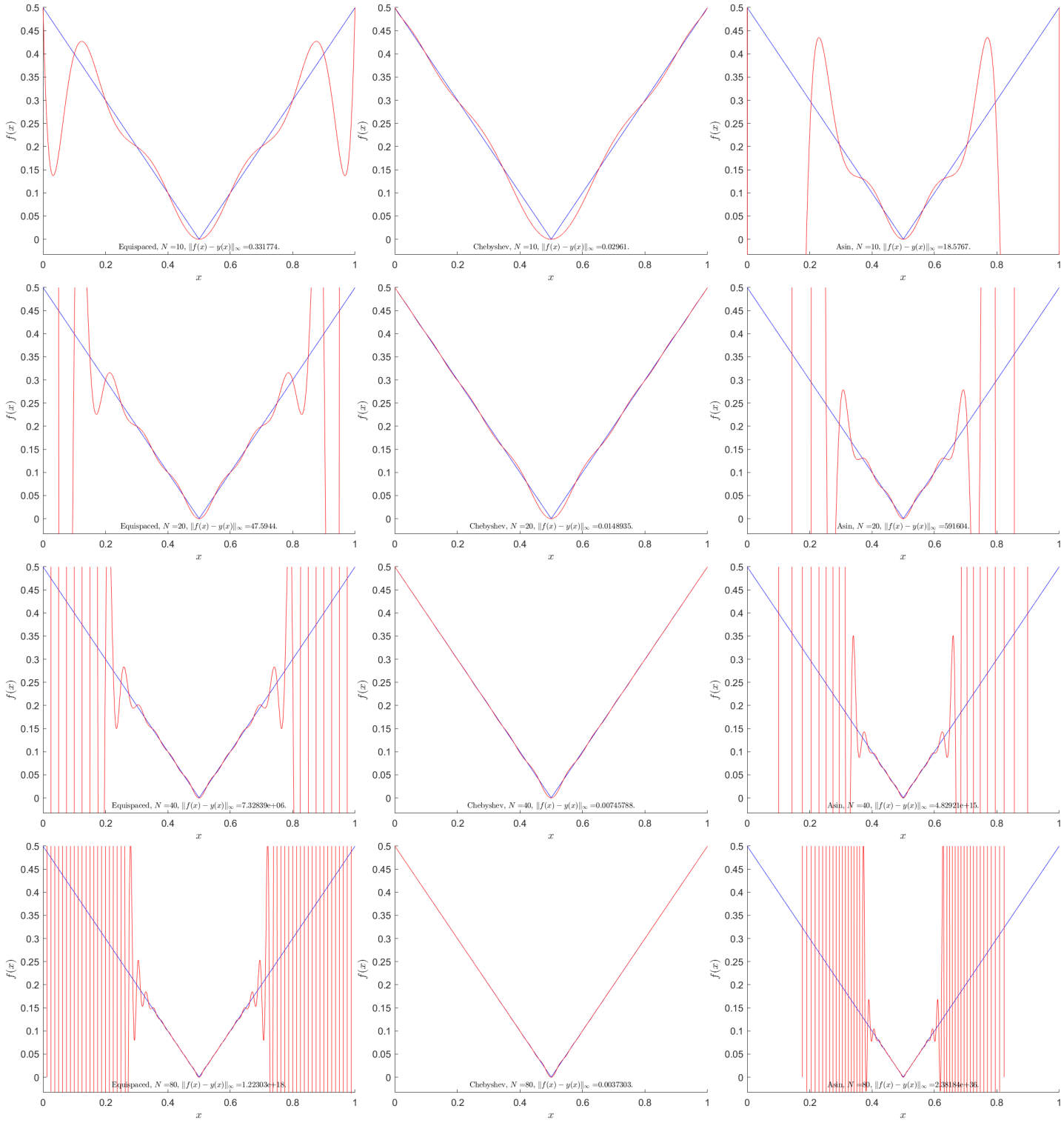

Figure 17. Results of Lagrange interpolation for 10, 20, 40 and 80 data points. The function is pictured with blue, its interpolant with red. First colomn corresponds to Equispaced data point distribution, second to Chebyshev and third to Asin.

3.2 Hermit interpolant

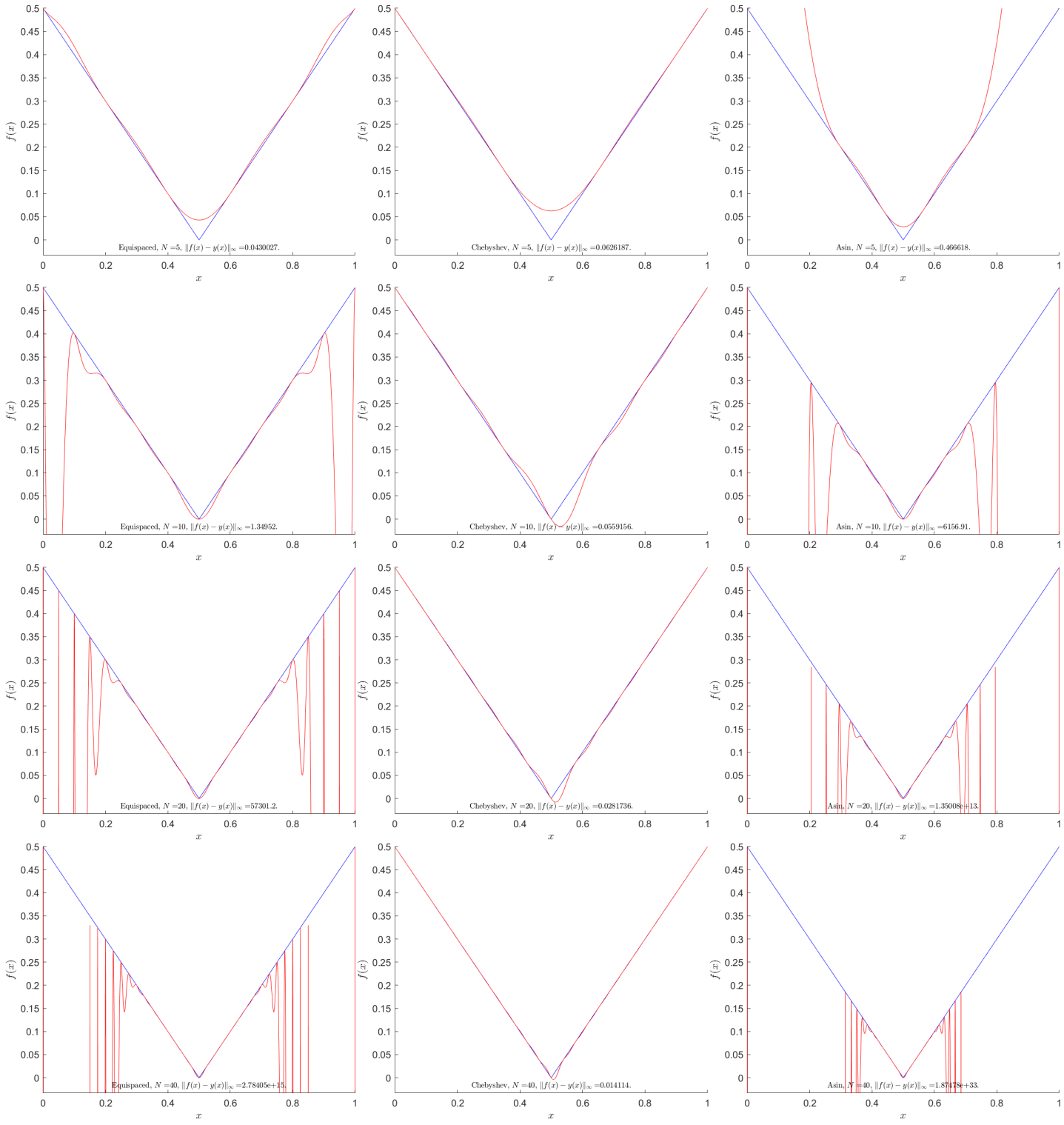

Figure 18. Results of Hermit interpolation for 5, 10, 20 and 40 data points. The function is pictured with blue, its interpolant with red. First colomn corresponds to Equispaced data point distribution, second to Chebyshev and third to Asin.

3.3 Accuracy analysis

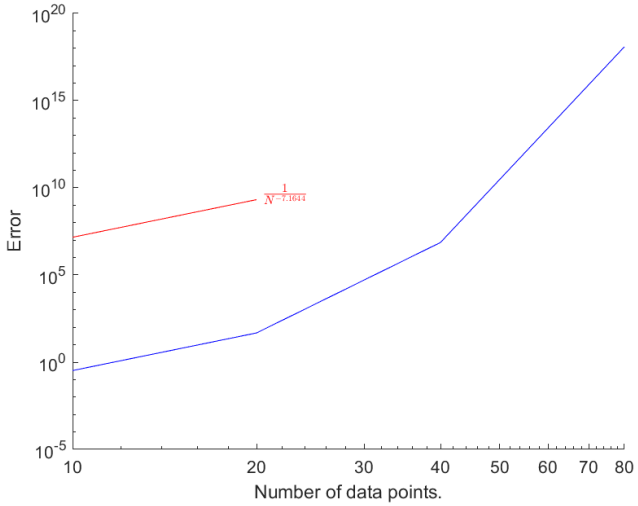

Figure 19. Dependence of error on the number of data points for Lagrange interpolant and Equispaced point distribution.

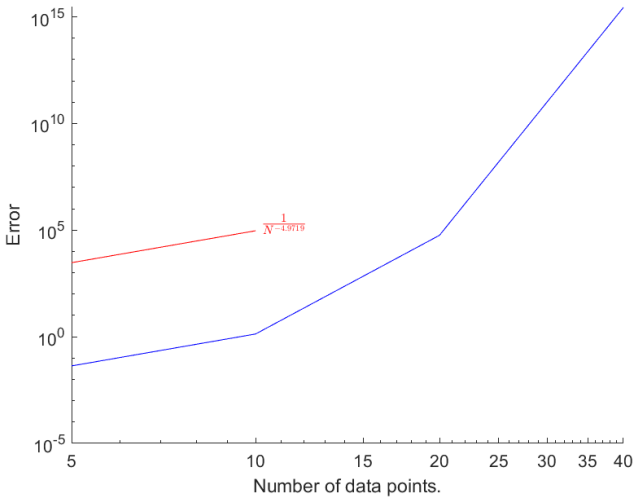

Figure 20. Dependence of error on the number of data points for Hermit interpolant and Equispaced point distribution.

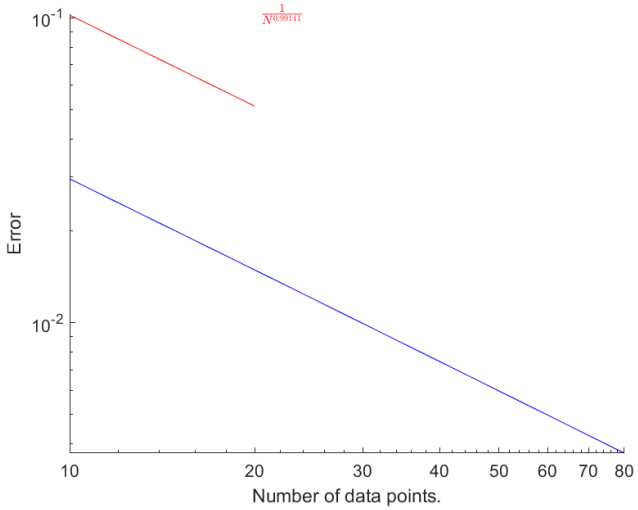

Figure 21. Dependence of error on the number of data points for Lagrange interpolant and Chebyshev point distribution.

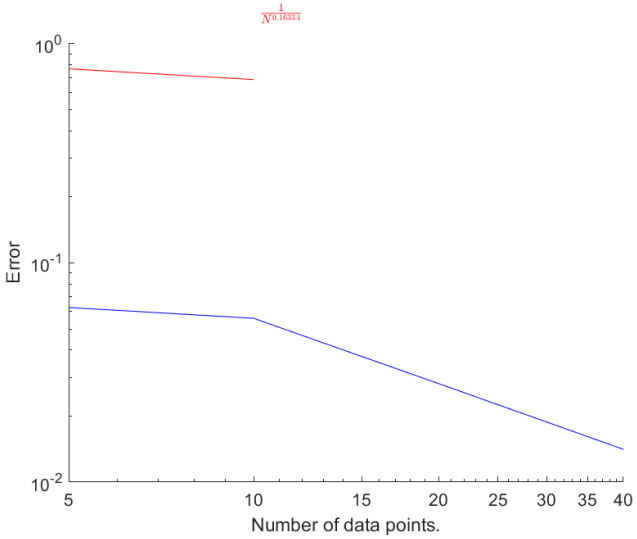

Figure 22. Dependence of error on the number of data points for Hermit interpolant and Chebyshev point distribution.

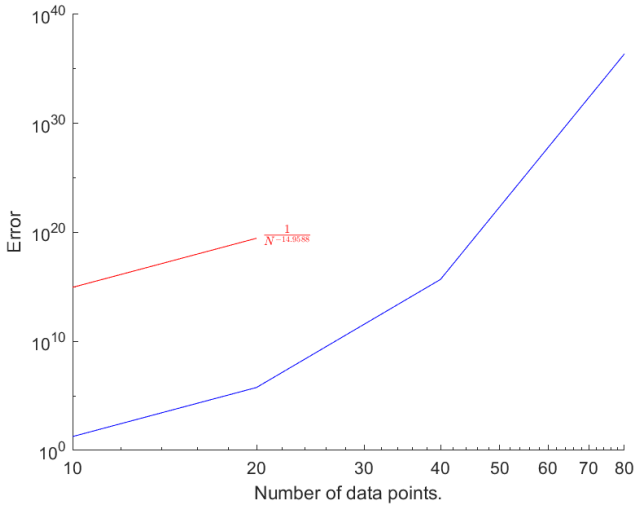

Figure 23. Dependence of error on the number of data points for Lagrange interpolant and Asin point distribution.

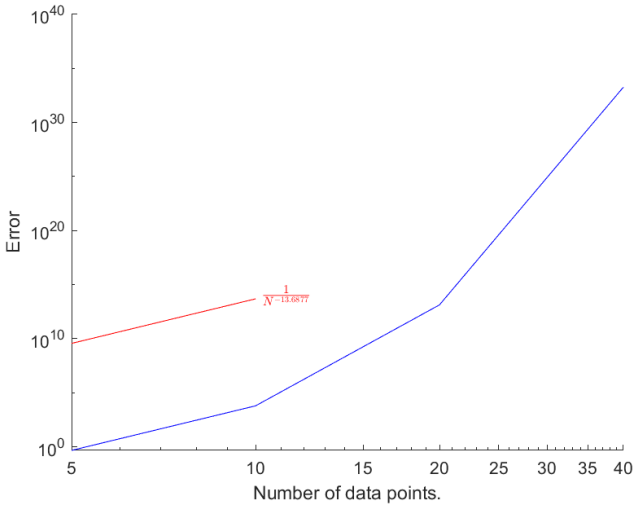

Figure 24. Dependence of error on the number of data points for Hermit interpolant and Asin point distribution.

New phenomenon can be seen: for $N = 5$ Hermit interpolation using Equispaced distribution is actually more accurate than Chebyshev. This is most likely the consequence of non-smoothness at $x = \frac{1}{2}$.

4 $\sqrt{1-x^2}$

4.1 Lagrange interpolant

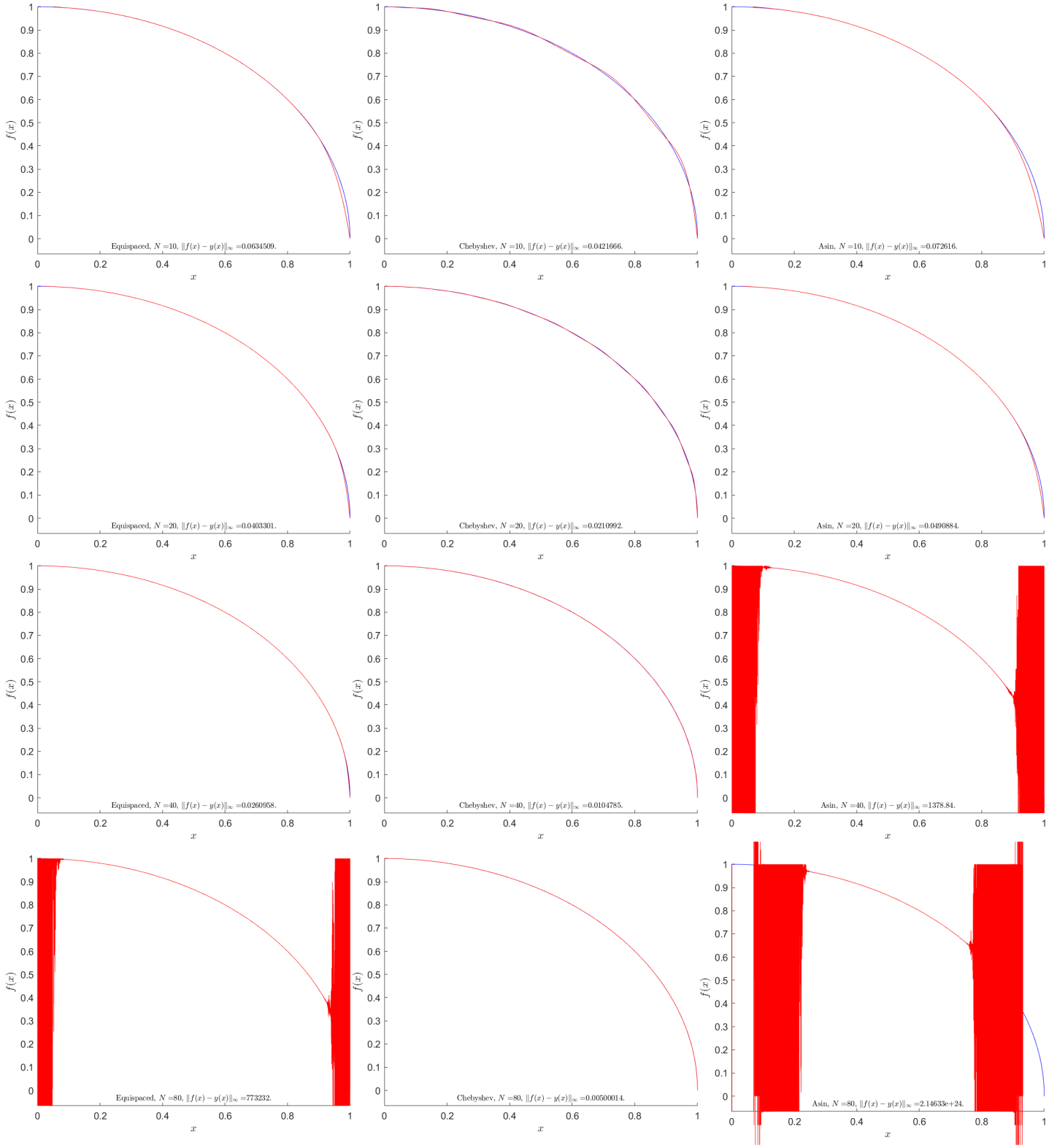

Figure 25. Results of Lagrange interpolation for 10, 20, 40 and 80 data points. The function is pictured with blue, its interpolant with red. First colomn corresponds to Equispaced data point distribution, second to Chebyshev and third to Asin.

4.2 Hermit interpolant

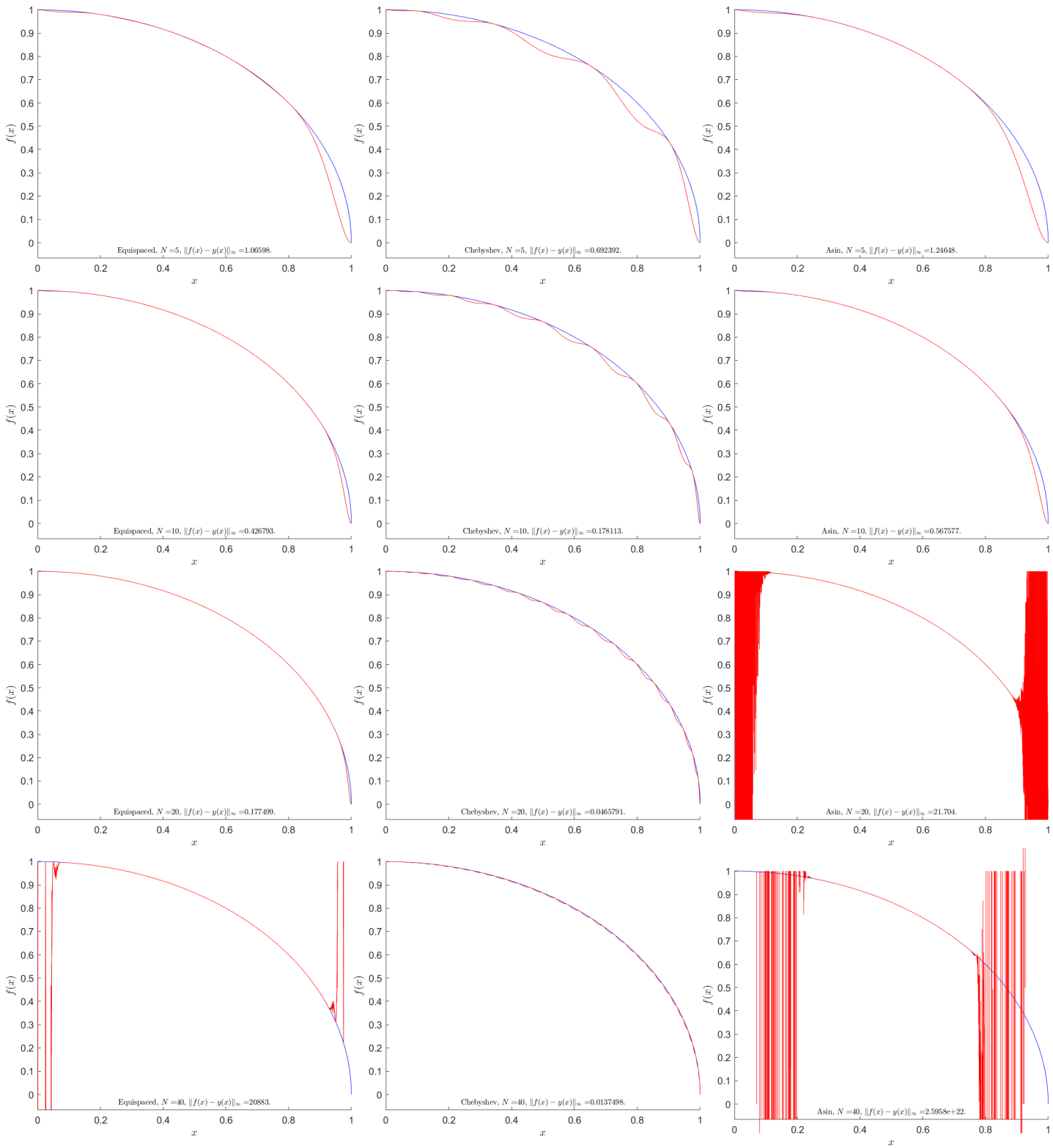

Figure 26. Results of Hermit interpolation for 5, 10, 20 and 40 data points. The function is pictured with blue, its interpolant with red. First colomn corresponds to Equispaced data point distribution, second to Chebyshev and third to Asin.

4.3 Accuracy analysis

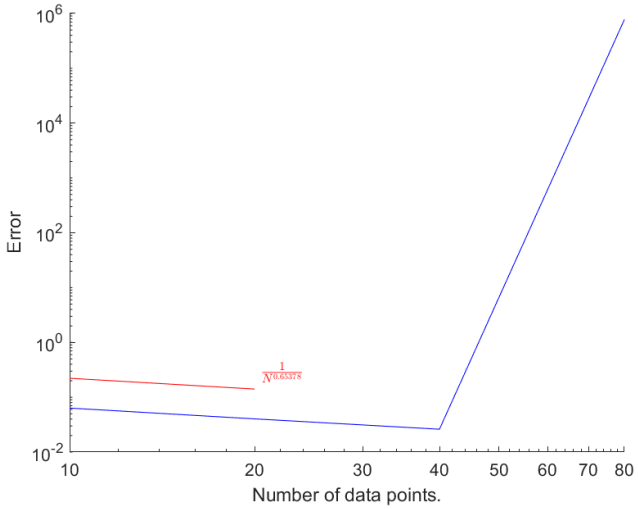

Figure 27. Dependence of error on the number of data points for Lagrange interpolant and Equispaced point distribution.

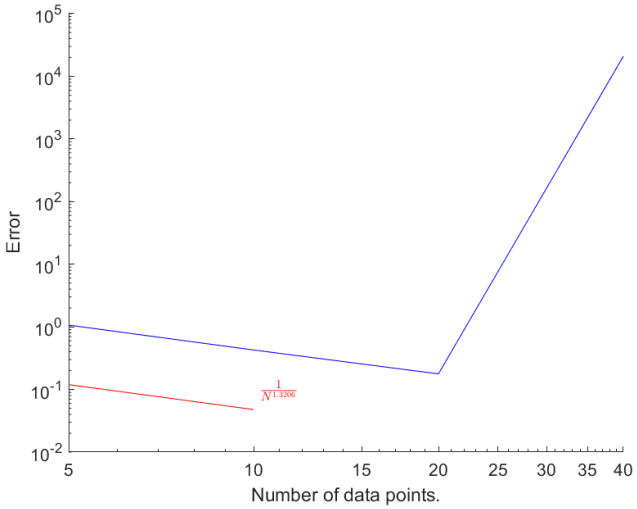

Figure 28. Dependence of error on the number of data points for Hermit interpolant and Equispaced point distribution.

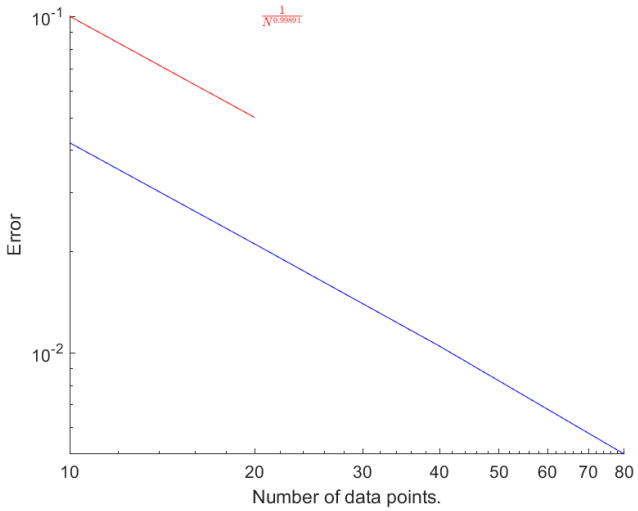

Figure 29. Dependence of error on the number of data points for Lagrange interpolant and Chebyshev point distribution.

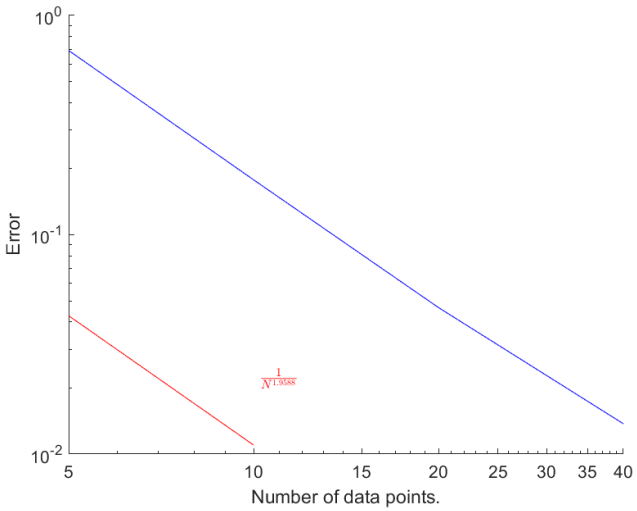

Figure 30. Dependence of error on the number of data points for Hermit interpolant and Chebyshev point distribution.

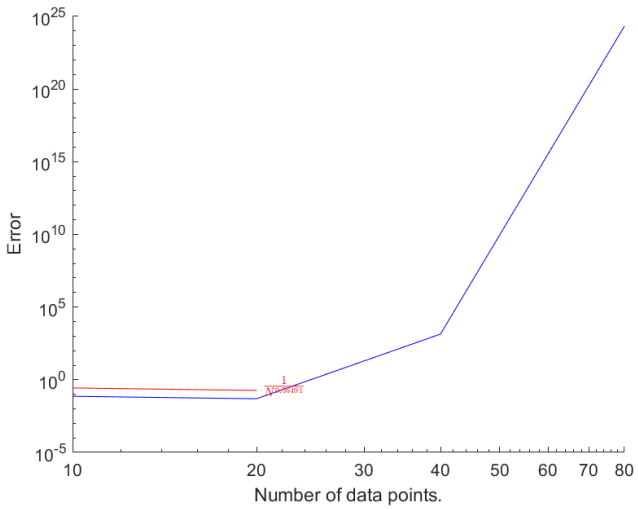

Figure 31. Dependence of error on the number of data points for Lagrange interpolant and Asin point distribution.

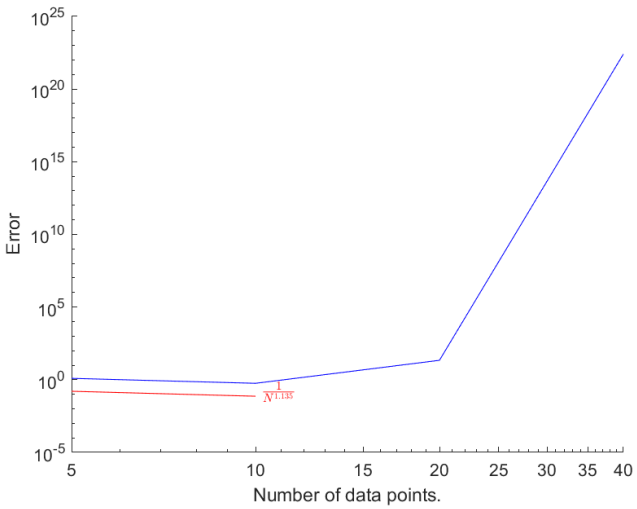

Figure 32. Dependence of error on the number of data points for Hermit interpolant and Asin point distribution.

Mostly the same dependencies can be seen for this function. However, it should be noted that for Hermit interpolation the rightmost point was mooved from $x = 1$ to $x = 1.0001$, because the first derivative at $x = 1$ is infinite.

Part II
Cubic spline interpolation

5 Parametrization

Cubic spline interpolation of an ellipse:

$$x^2 + \frac{y^2}{2} = 1, \tag{1}$$

is considered. Since the curve satisfying Eq.(1) can not be expressed in a form $y(x)$, we will work with its parametrization $(x(t), y(t))$. A set of data points is generated from:

$$\begin{cases} x = cos(t), \\ y = \sqrt{2}sin(t), \end{cases} \tag{2}$$

where $t \in [0, 2\pi + \delta]$. The interpolation was performed for N =9, 13, 17, and 21 data points, extension of the interval $\delta = \frac{2\pi}{N-1}$ is introduced to apply periodic boundary conditions: $f''(N-1) = f(0), \quad f''(N) = f(1)$.

6 Results

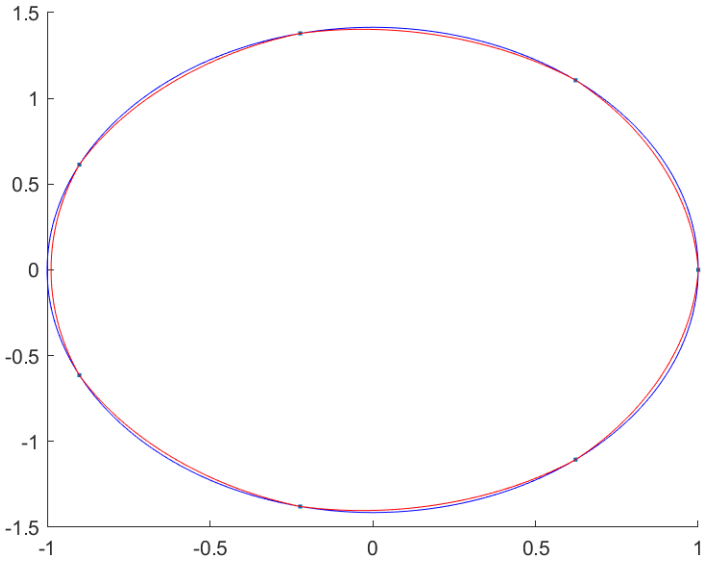

Figure 33. Interpolant for $N = 9$.

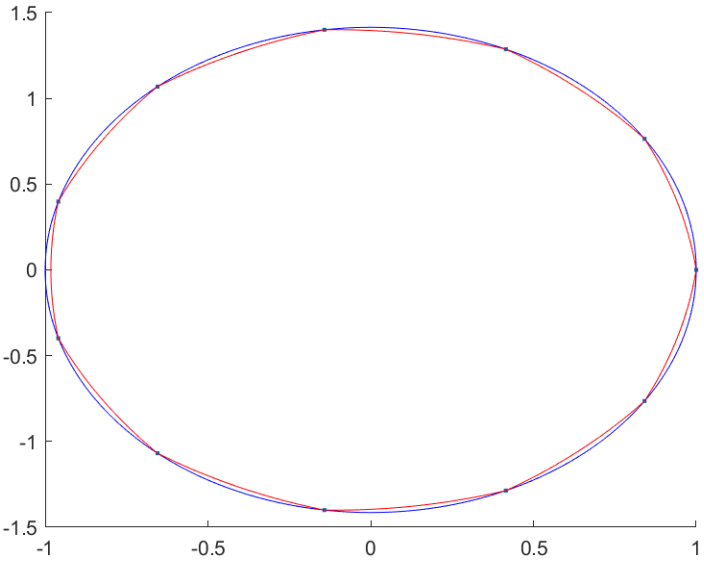

Figure 34. Interpolant for $N = 13$.

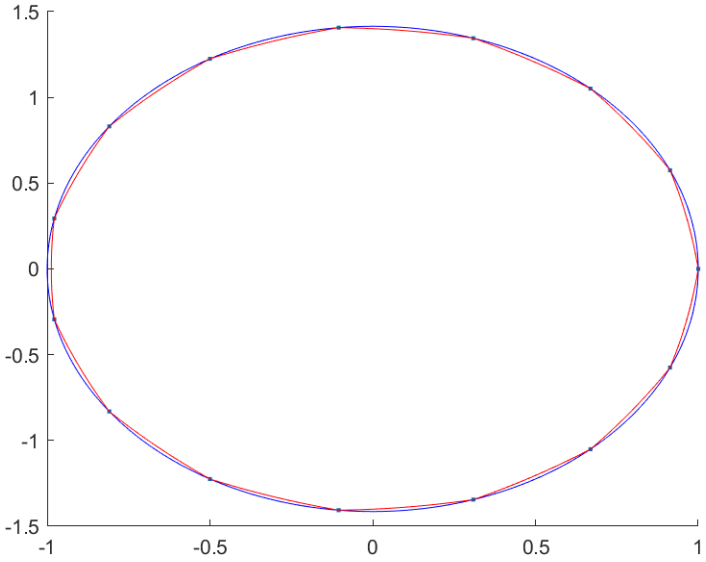

Figure 35. Interpolant for $N = 17$.

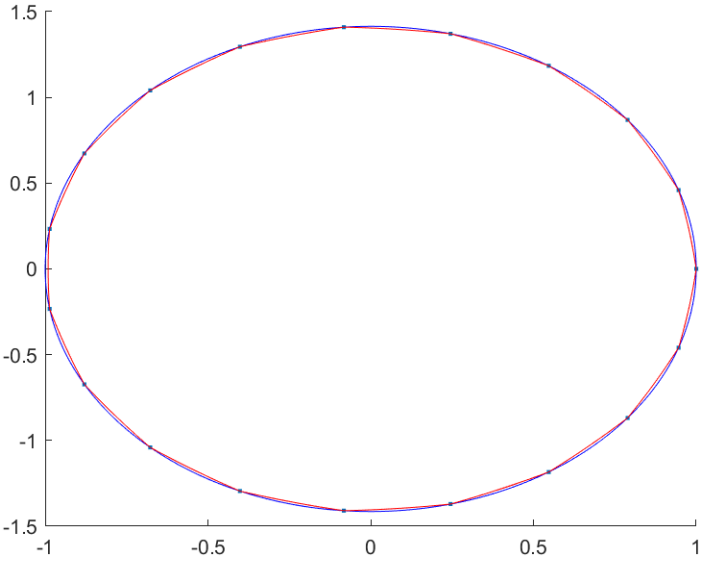

Figure 36. Interpolant for $N = 21$.

Figure 37. Cubic spline interpolant is pictured with red and the actual function with blue.

Part III
Finite difference and Padé approximation

7 Finite difference

The most accurate finite difference formula for $f''(x_i)$ of a function $f(x)$ known at points x_{i-1}, x_i, x_{i+1}, x_{i+2}, and x_{i+3} is considered. The points are equispaced with distance h between them. The problem can be reduced to finding coefficients a, b, c, d, and e such that

$$f''(x_i) = af(x_{i-1}) + bf(x_i) + cf(x_{i+1}) + df(x_{i+2}) + ef(x_{i+3}) + Ch^p + O(h^{p+1}) \tag{3}$$

with maximum possible p. By substituting each function with its Taylor series expansion around x_i and requiring the coefficient in front of second derivative to be qual 1 and all other 0 the following equations for a, b, c, d, and e can be obtained:

$$\begin{cases} a+b+c+d+e=0, \\ -h\cdot a + h\cdot c + 2\cdot h\cdot d + 3\cdot h\cdot e = 0, \\ \frac{h^2}{2}\cdot a + \frac{h^2}{2}\cdot c + 2\cdot h^2\cdot d + \frac{9\cdot h^2}{2}\cdot e = 1, \\ -\frac{h^3}{6}\cdot a + \frac{h^3}{6}\cdot c + \frac{4\cdot h^3}{3}\cdot d + \frac{9\cdot h^3}{2}\cdot e = 0, \\ \frac{h^4}{24}\cdot a + \frac{h^4}{24}\cdot c + \frac{2\cdot h^4}{3}\cdot d + \frac{27\cdot h^4}{8}\cdot e = 0, \end{cases} \tag{4}$$

By substituting the solution of System(4) into Eq.(3) we obtain:

$$f_i'' = \frac{11f_{i-1} - 20f_i + 6f_{i+1} + 4f_{i+2} - f_{i+3}}{12h^2} + \frac{h^3}{12} + O(h^4) \tag{5}$$

8 Padé approximation

The most accurate Padé approximation for $f'(x_i)$ of a function $f(x)$ known at points x_{i-2}, x_{i-1}, and x_i is considered. The points are equispaced with distance h between them. The problem can be reduced to finding coefficients a, b, c, d, and e such that

$$h(af'(x_{i-2}) + bf'(x_{i-1}) + f'(x_i)) = cf(x_{i-2}) + df(x_{i-1}) + ef(x_i) + Ch^p + O(h^{p+1}) \tag{6}$$

with maximum possible p. By substituting each function with its Taylor series expansion around x_i and requiring the coefficient in front of each derivative from the right side to be qual to the coefficient in front of the same derivative from the left side following equations for a, b, c, d, and e can be obtained:

$$\begin{cases} -c-d-e == 0, \\ 2\cdot c\cdot h + d\cdot h + h\cdot(a+b+1) = 0, \\ -h\cdot(2\cdot a\cdot h + b\cdot h) - 2\cdot c\cdot h^2 - \frac{d\cdot h^2}{2} = 0, \\ h\cdot(2\cdot a\cdot h^2 + \frac{b\cdot h^2}{2}) + \frac{4\cdot c\cdot h^3}{3} + \frac{d\cdot h^3}{6} = 0, \\ -h\cdot(\frac{4\cdot a\cdot h^3}{3} + \frac{b\cdot h^3}{6}) - \frac{2\cdot c\cdot h^4}{3} - \frac{d\cdot h^4}{24} = 0, \end{cases} \tag{7}$$

By substituting the solution of System(7) into Eq.(6) we obtain:

$$h(f'(x_{i-2}) + 4f'(x_{i-1}) + f'(x_i)) = -3f(x_{i-2}) + 3f(x_i) + \frac{h^5}{30} + O(h^6) \tag{8}$$

Part IV

Numeric integration

Different formulas for numeric integraion of

$$\int_0^1 \left(\frac{1}{(x-1)^2+0.002}+\frac{1}{(x-0.2)^2+0.005}-5\right)\cdot dx = \frac{atan(\frac{1}{\sqrt{0.002}})}{\sqrt{0.002}}+\frac{atan(\frac{0.8}{\sqrt{0.005}})}{\sqrt{0.005}}+\frac{atan(\frac{0.2}{\sqrt{0.005}})}{\sqrt{0.005}}-5 \tag{9}$$

are considered. In each method except for adaptive quadrature the interval is divided into N equal segments of length $h=\frac{1}{N}$ and results are obtained for N =8, 16, 32, 64, 128, 256.

9 Trapezoidal Rule

$$I \approx h\left(\frac{f_0+f_N}{2}+\sum_{j=1}^{N-1} f_j\right)$$

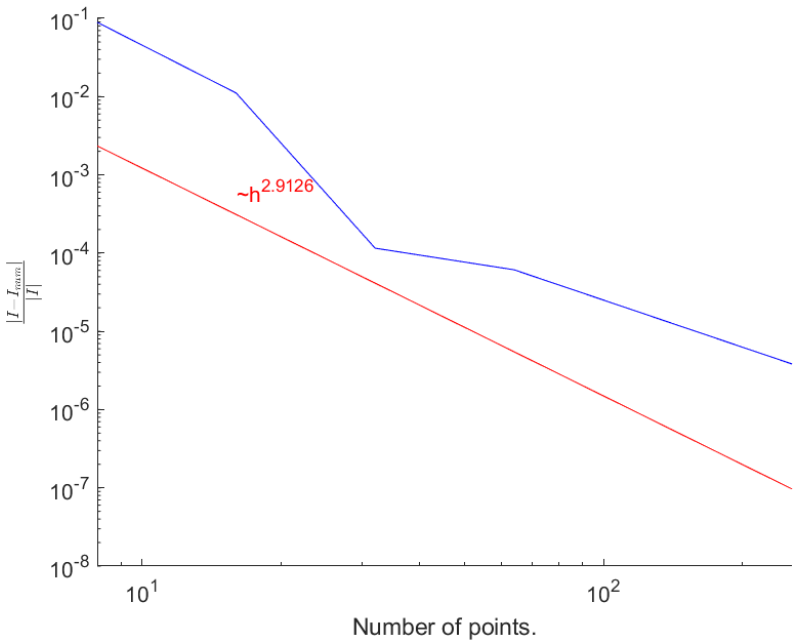

Figure 38. Trapesoidal Rule. Error vs N is pictured with blue and approximation of order of accuracy with red.

The results show that the method is at least second order accurate for the considered integral.

10 Simpson's Rule

$$I \approx \frac{h}{3}\left(f_0+f_N+4\cdot \sum_{\substack{j=1\\ j=odd}}^{N-1} f_j+2\cdot \sum_{\substack{j=1\\ j=even}}^{N-1} f_j\right)$$

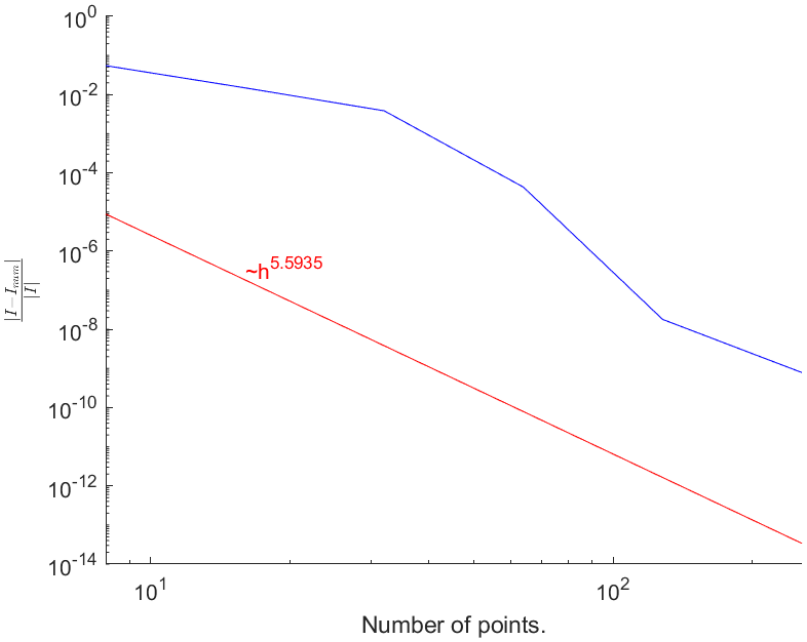

Figure 39. Simpson's Rule. Error vs N is pictured with blue and approximation of order of accuracy with red.

The results show that the method is even higher than third order accurate for the considered integral.

11 Trapezoidal Rule with End-Correction

$$I \approx h\left(\frac{f_0 + f_N}{2} + \sum_{j=1}^{N-1} f_j\right) - \frac{h^2}{12}(f'_N - f'_0)$$

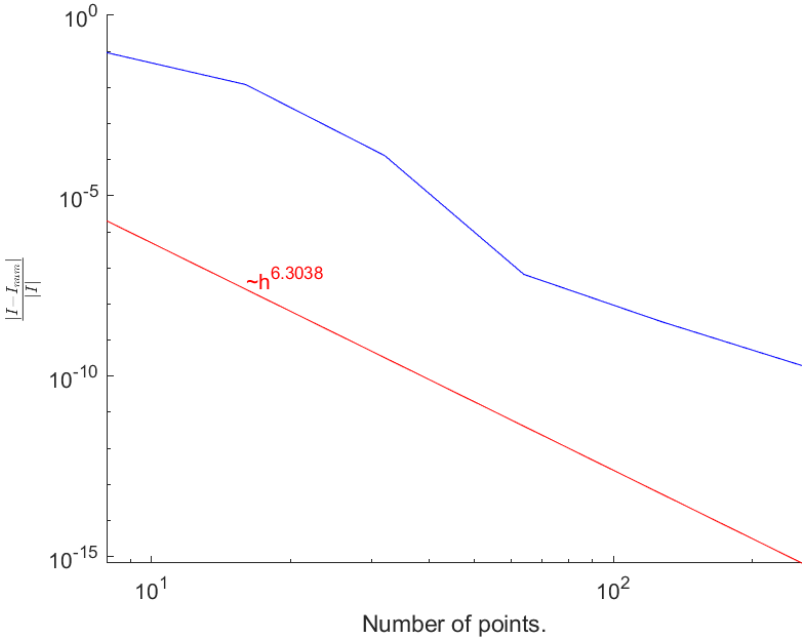

Figure 40. Trapezoidal with End=Correction Rule. Error vs N is pictured with blue and approximation of order of accuracy with red.

The results show that the method is even higher than forth order accurate for the considered integral.

12 Adaptive Quadrature

The approximation of the integral over a segment $[a, b]$ is obtained using Rectangular Rule: $\int_a^b f(x)\,dx \approx (b-a)\cdot f(\frac{a+b}{2}) = I_{[a,b]}$. The error of approximation is estimated using Richardson Extrapolation. If the value of $|I_{[a,b]} - (I_{[a,\frac{a+b}{2}]} + I_{[\frac{a+b}{2},b]})|$ is less than some predetermined tolerance, tol, $I_{[a,b]}$ is taken as the approximation, else the same prosedure is performed for ($I_{[a,\frac{a+b}{2}]}$ and $I_{[\frac{a+b}{2},b]}$) with $\widetilde{tol} = \frac{tol}{2}$, the point $x = \frac{a+b}{2}$ is added to the resulting distribution of dividing points. The recursive procedure is started with $[a, b] = [0, 1]$. Numerical calculations were conducted for $tol = 10^{-1},\ 10^{-3},\ 10^{-5},\ 10^{-7}$.

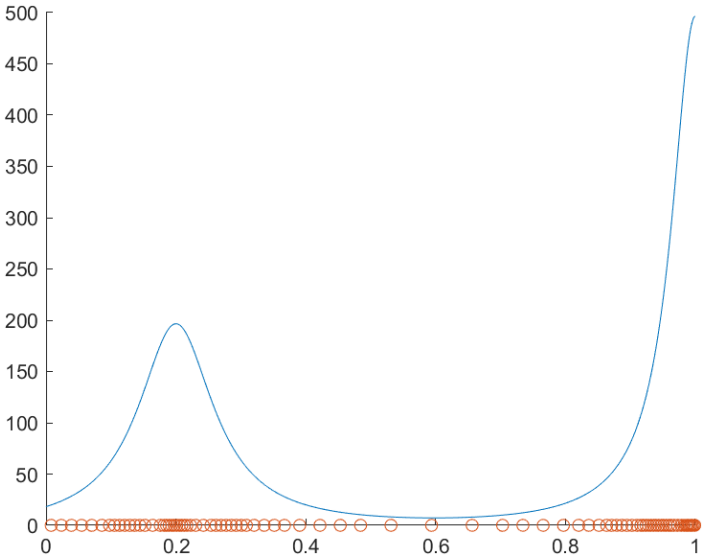

Figure 41. The function is pictured with blue line and point distribution for $tol = 10^{-1}$ with red circles.

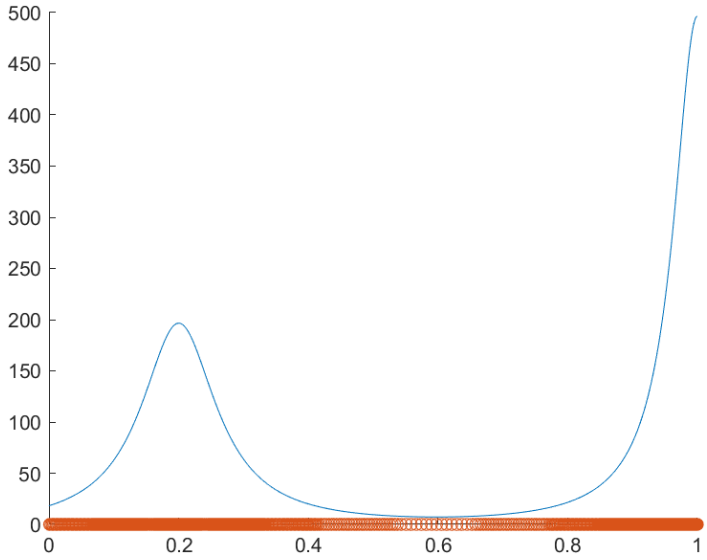

Figure 42. The function is pictured with blue line and point distribution for $tol = 10^{-3}$ with red circles.

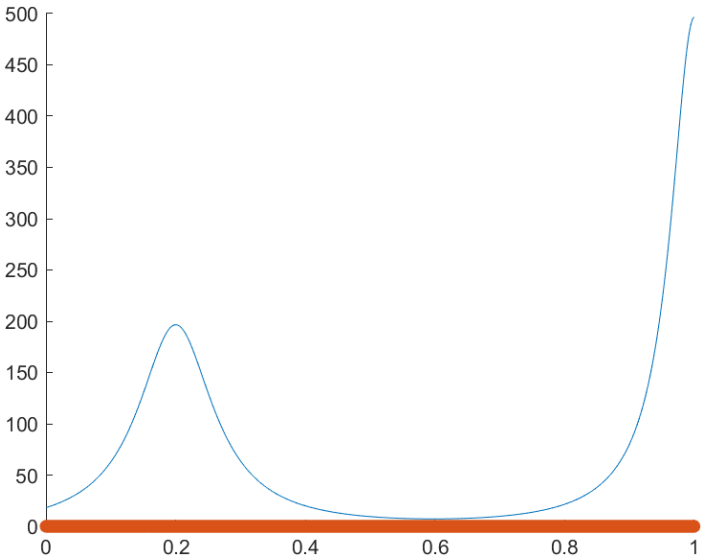

Figure 43. The function is pictured with blue line and point distribution for $tol = 10^{-5}$ with red circles.

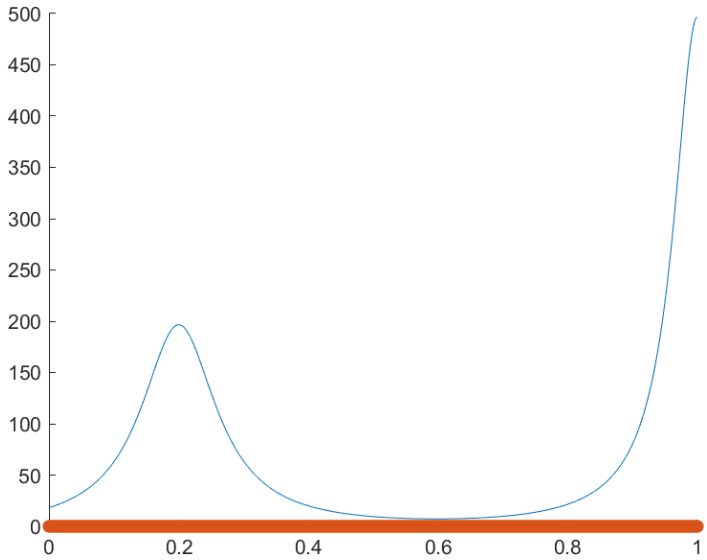

Figure 44. The function is pictured with blue line and point distribution for $tol = 10^{-7}$ with red circles.

The leading error term for Rectangular Rule depends on the second derivative of the function. It is natural that the distribution of points for adaptive quadrature follows it.

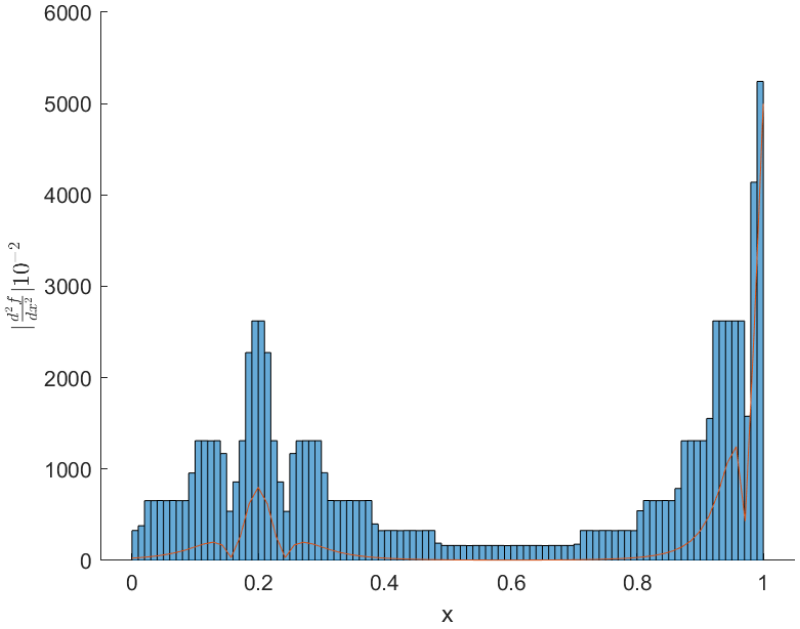

Figure 45. Histogram with 100 equispaced bins is pictured with blue and $|f''(x)| \cdot 10^{-2}$ with red.

Part V

Numeric integration of improper integrals

13 Semi-Infinite intervals

The following formula for numerical integration of improper integrals is considered: $\int_0^\infty e^{-x} f(x)\ dx \approx \sum_{j=0}^{N} \omega_j f(x_j)$, where x_j and ω_j are zeros and weight factors of Laguerre polinomial corresponding to the chosen number of points N. Numerical integration for N =2, 3, 4, 5 will be conducted.

13.1 $\int_0^\infty e^{-10x} sin(x)\ dx$

$$I = \int_0^\infty e^{-10x} sin(x)\ dx = \frac{1}{10}\int_0^\infty e^{-10x} cos(x)\ dx = \frac{1}{100} - \frac{1}{100}\int_0^\infty e^{-10x} sin(x)\ dx => I = \frac{1}{101}, \tag{10}$$

$$\int_0^\infty e^{-10x} sin(x)\ dx = \frac{1}{10}\int_0^\infty e^{-t} sin(\frac{t}{10})\ dt \approx \sum_{j=0}^{N} \omega_j sin(\frac{x_j}{10}). \tag{11}$$

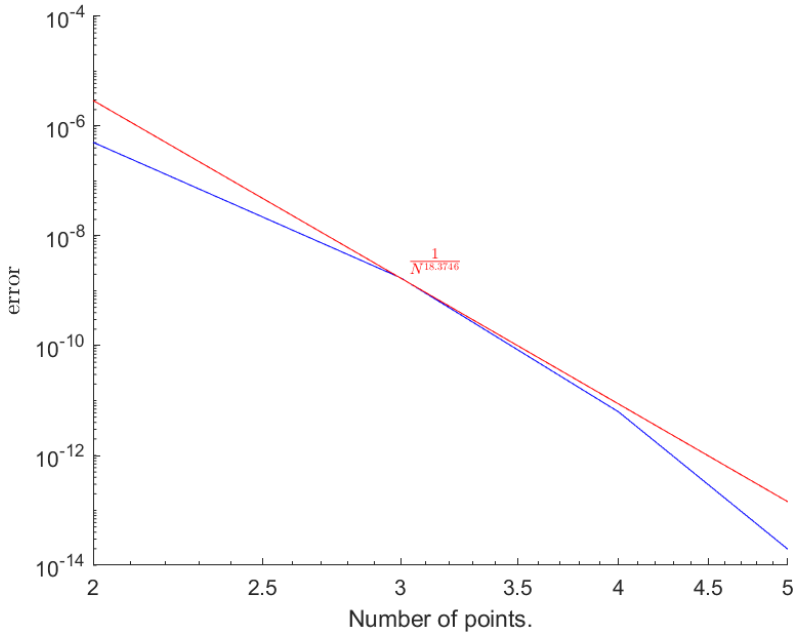

Figure 46. Error vs N is pictured with blue and approximation of order of accuracy with red.

13.2 $\int_0^\infty \frac{e^{-x}}{1+e^{-2x}}\ dx$

$$I = \int_0^\infty \frac{e^{-x}}{1+e^{-2x}}\ dx = -\int_0^\infty \frac{1}{1+e^{-2x}}\ de^{-x} = atan(1) = \frac{\pi}{4}, \tag{12}$$

$$\int_0^\infty \frac{e^{-x}}{1+e^{-2x}}\ dx \approx \sum_{j=0}^{N} \omega_j \frac{1}{1+e^{-2x_j}}. \tag{13}$$

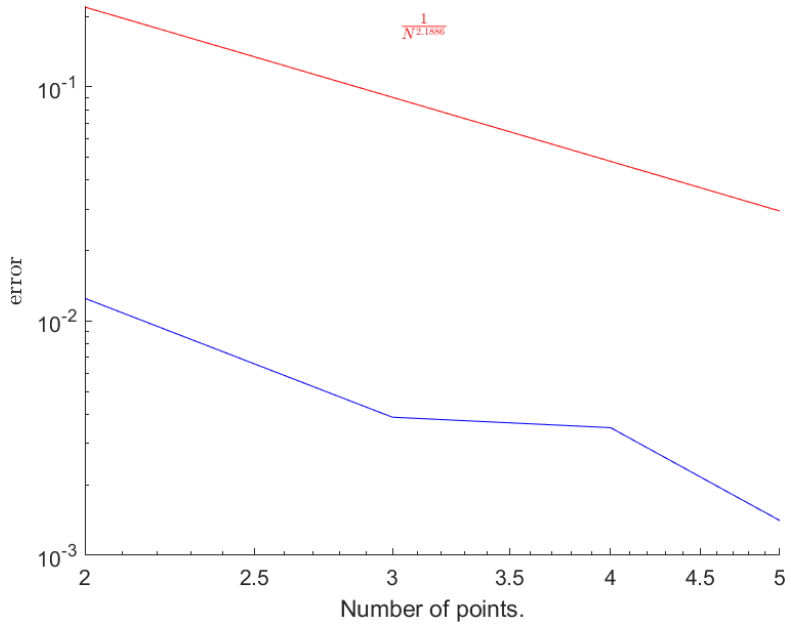

Figure 47. Error vs N is pictured with blue and approximation of order of accuracy with red.

14 Infinite intervals

The following formula for numerical integration of improper integrals is considered: $\int_{-\infty}^{\infty} e^{-x^2} f(x)\ dx \approx \sum_{j=0}^{N} \omega_j f(x_j)$, where x_j and ω_j are zeros and weight factors of Hermit polinomial corresponding to the chosen number of points N. Numerical integration for N =2,3,4,5 will be conducted.

14.1 $\int_{-\infty}^{\infty} |x| e^{-3x^2}\ dx$

$$I = \int_{-\infty}^{\infty} |x| e^{-3x^2}\ dx = \int_{0}^{\infty} e^{-3x^2}\ dx^2 = \frac{1}{3}, \tag{14}$$

$$\int_{-\infty}^{\infty} |x| e^{-3x^2}\ dx = \frac{1}{3} \int_{-\infty}^{\infty} |t| e^{-t^2}\ dt \approx \sum_{j=0}^{N} \omega_j \frac{1}{3} |x_j|. \tag{15}$$

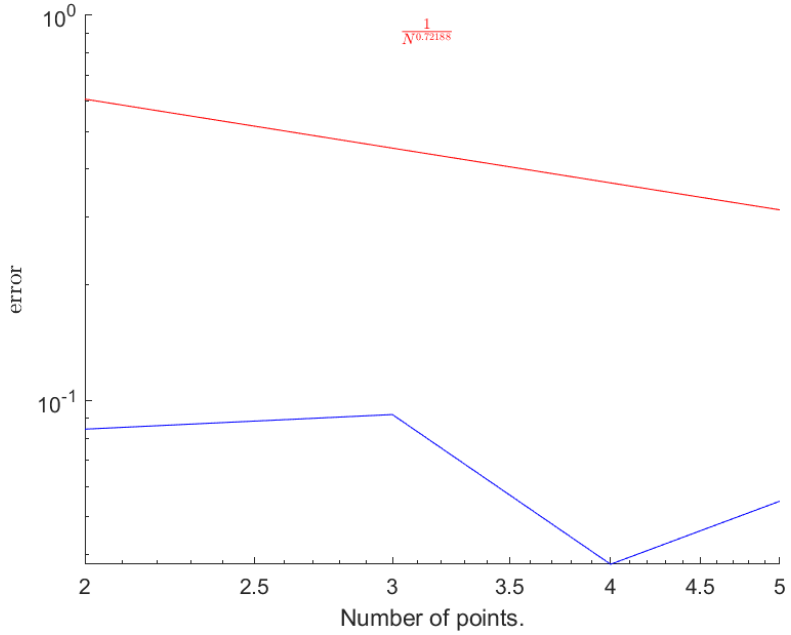

Figure 48. Error vs N is pictured with blue and approximation of order of accuracy with red.

14.2 $\int_{-\infty}^{\infty} e^{-x^2} cos(x)\ dx$

$$I(\alpha) = \int_{-\infty}^{\infty} e^{-x^2} cos(\alpha x)\ dx, \quad I(0) = \int_{-\infty}^{\infty} e^{-x^2}\ dx = \sqrt{\pi} \tag{16}$$

$$I'(\alpha) = -\int_{-\infty}^{\infty} x e^{-x^2} sin(\alpha x)\ dx = -\frac{\alpha}{2}\int_{-\infty}^{\infty} e^{-x^2} cos(\alpha x)\ dx = -\frac{\alpha}{2} I(\alpha), \tag{17}$$

$$I'(\alpha) = -\frac{\alpha}{2} I(\alpha) \quad => \quad I(\alpha) = I(0) e^{\frac{-\alpha^2}{4}} \quad => \quad \int_{-\infty}^{\infty} e^{-x^2} cos(x)\ dx = I(1) = \frac{\sqrt{\pi}}{e^{\frac{1}{4}}}$$

$$\int_{-\infty}^{\infty} e^{-x^2} cos(x)\ dx \approx \sum_{j=0}^{N} \omega_j cos(x_j). \tag{18}$$

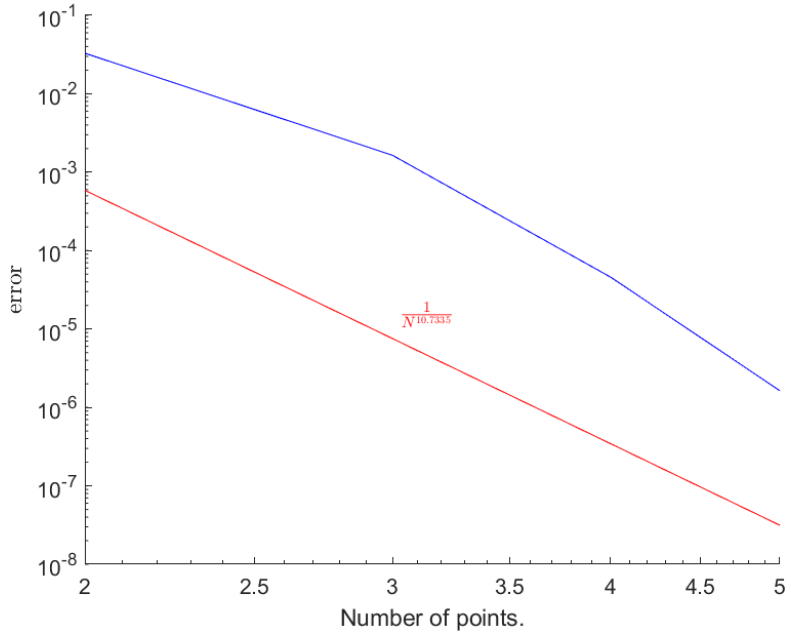

Figure 49. Error vs N is pictured with blue and approximation of order of accuracy with red.